ABSTRACT

THE APPLICATION OF MODIFIED LINEAR ELASTIC FRACTURE MECHANICS (LEFM) AND ITS IMPLICATION FOR TEAR STRENGTH DEVELOPMENT OF FIBROUS MATERIALS

by Ziyang Zhang

Linear Elastic Fracture Mechanics (LEFM) has been modified to account for the role of inherent fracture processing zone in failure of fibrous materials. The presented study further validates the theory using both prepared handsheets with different pressing conditions and literature reported handsheet tensile strength data under different notch size. The analysis shows that modified LEFM can capture the trend of tensile strength as functions of notch size. To further expand the application of the model, we used a simple shifting manipulation coupled with a fitting procedure to indirectly determine characteristic fracture processing zone length. After the treatment, all the tensile strength data were fitted into a unified fracture model. The results show that increasing porosity or decreasing density leads to increase of fracture processing zone length. Lastly, we evaluated the role of tensile strength in affecting the tear strength. We found that tear strength reaches a maximum value as tensile strength increases but drops dramatically once tensile strength or breaking length reaches a critical value for softwood based handsheets. The implication of this results suggests that one should consider the nature of the fibers when preparing high tensile strength and tear strength fibrous materials.

THE APPLICATION OF MODIFIED LINEAR ELASTIC FRACTURE MECHANICS (LEFM) AND ITS IMPLICATION FOR TEAR STRENGTH DEVELOPMENT OF FIBROUS MATERIALS

A Thesis

Submitted to the

Faculty of Miami University

in partial fulfillment of

the requirements for the degree of

Master of Science

by

Ziyang Zhang

Miami University

Oxford, Ohio

2020

Advisor: Professor Douglas W. Coffin

Reader: Professor Jessica L. Sparks

Reader: Professor Shashi Lalvani

This Thesis titled

THE APPLICATION OF MODIFIED LINEAR ELASTIC FRACTURE MECHANICS (LEFM) AND ITS IMPLICATION FOR TEAR STRENGTH DEVELOPMENT OF FIBROUS MATERIALS

by

Ziyang Zhang

has been approved for publication by

The College of Engineering and Computing

and

Department of Chemical, Paper, and Biomedical Engineering

Douglas Coffin

Jessica Sparks

Shashi Lalvani

Table of Contents

List of Figures

Acknowledgements

It has been a unique experience for me starting on the first day enrolling in chemical engineering major in Miami University. I met with Prof. Coffin and he showed me some interesting ideas including making paper-based cellphone and fracture modeling. I was amazed by his brilliant idea and chose the one that I was interested in. My life went a detour when I started graduate school in Miami University. I have been struggling during that time dealing with family issues and I was depressed at that time. I had been introverted but Dr. Coffin had shown tremendous patience to me. Even after I went to Worcester Polytechnic Institute to pursue doctoral study, he traded email with me about the original research idea he came up. With that being said, I greatly appreciate Dr. Coffin for his generous support and long-term patience.

I would like to thank my wife (Yuxin) who was also a graduate student in Miami University. I sincerely apologized for my inexperience in dealing with family issues. I am glad that we have been through those and we will be together for lifetime.

I also thank paper and chemical engineering department for their financial support and recommendation letter for my doctoral study. I enjoyed the days working with Prof. Sparks and Prof. Lalvani.

Lastly, I would like to thank my family, including my Mom, Dad and two lovely brothers for supporting me along the way.

1. Introduction

Fibrous materials, including polymer fibers, tissue papers and towers and graphene fiber-based materials have a wide range of applications from biomedical devices fabrication to packaging industries.[1-5] Of those materials, cellulose-based paper materials have attracted much attention not only due to its advantages such as abundant source, ease of processing and sustainability, but also continued technology and processing technique to improve its mechanical properties.[6] For example, Motamedian et al.[7] optimized the refining process by introducing fine nano-fibers for enhanced fiber bonding. Li et al.[8] have used the polyelectrolyte and its electrostatic attraction to fabricate high-strength cellulose based sheets. Peng et al.[9] used a layer-by-layer assembly technique to compress polyelectrolytes with lignosulfonates-amine. Their lignin-based fibers and sheets not only possess high mechanical strength, but also high hydrophobicity, increasing the possibility for commercialization.

One of the main challenges when using cellulose-based paper materials is that the mechanical strength, such as tensile strength and tear strength, are difficult to predict or estimate.[10] Meanwhile, unlike solid materials where defects or cracks can be easily detected by non-destructive testing method such as eddy-current, magnetic-particle, liquid penetrant, fibrous materials such as tissue papers consists of numerous fibers and the cracks or defects are basically spread everywhere.[11-13] Therefore, current technology is limited to characterize or predict tensile strength of paper products.

Various theories and models have been proposed over the last few decades to understand the fracture mechanism of paper materials.[14-19] Those theories typically fall into three different categories of material fractures, namely, opening mode, sliding mode and tearing mode. Most of the time, those three modes could occur at the same time, as shown in **Figure 1**. For example, Okaniwa [20] has shown that J-integral can be used for characterizing fracture toughness and his method can differentiate handsheets prepared under different beating/conditions. Some studies used LEFM to characterize the fracture of papers.[17] But skepticism still remains regarding the feasibility of LEFM to characterize paper materials fracture toughness.

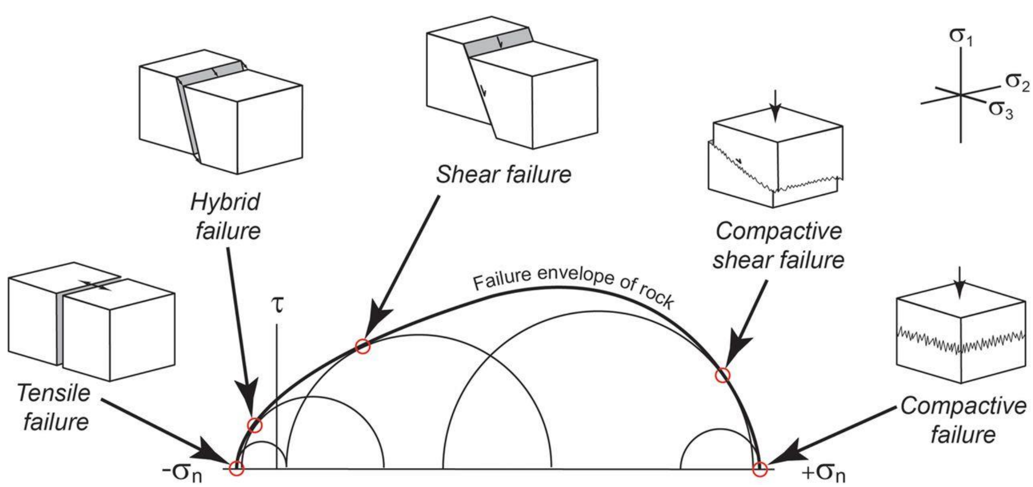

Figure 1. Materials failure type [21]

More advanced methods such as J-integral can work quite well in certain materials, especially for bleached softwood-based papers, but the complicated mathematical analysis often requires a lot of experimental data to validate, rendering it less effective.

LEFM has been proved useful for many applications including alloys and ceramics materials.[22-26] The main advantages of LEFM is its simplicity and accuracy, particularly for well-defined and structural materials. Accordingly, a recent study by Coffin et al.[27] have shown that although the original LEFM cannot directly apply to the paper materials, a modified model that includes the fracture processing zone can be used instead:

$$\frac{F}{F_0} = \begin{cases} 1 & \forall a \le d_s \\ \dfrac{f(d/w)}{f((a+d-d_s)/w)} \sqrt{\dfrac{d}{(a+d-d_s)}} & \forall d_s < a < w-2d \end{cases}$$

According to the modified linear elastic fracture model, F is the maximum force before the paper materials with notch fail and F_0 is the maximum force without a notch. w is the half sample width; a is the one-edged notch length and d_s is the structural fracture length, which is material dependent. By introducing the fracture processing zone, d, equation above can be used for characterizing tensile strength of paper materials. The $f(x)$ function is the geometric function and it depends on the testing configuration, as defined below:[27]

$$\text{for CNT:} \quad f(x) = \left(1 - 0.025x^2 + 0.06x^4\right)\sqrt{\sec\left(\pi x/2\right)}$$

$$\text{for DENT:} \quad f(x) = \left[1 + .122\cos^4\left(\pi x/2\right)\right]\sqrt{\frac{2\tan\left(\pi x/2\right)}{\pi x}}$$

$$\text{for SENT:} \quad f(x) = \frac{\left[0.752 + 2.02x + 0.37\left(1 - \sin\left(\pi x/2\right)\right)^3\right]}{\cos\left(\pi x/2\right)}\sqrt{\frac{2\tan\left(\pi x/2\right)}{\pi x}}$$

The established model works successfully in characterizing handsheets and various polymer-based materials, as shown by Coffin[27].

Despite that the established theory can be used to quantitatively fit tensile strength data well by using a proper fracture processing zone length, the feasibility of the theory to extract fracture processing zone parameter from handsheets prepared by different processing, e.g. wet-pressing, beating and refining, has not been pursued. Going beyond, tensile fracture often occurs with other type of failure such as tearing failure. The inter-connection between tensile strength and tear strength has been discussed in literature, but the role of fracture processing zone length in affecting both tensile strength and tear strength for various pump of different stiffness have not been studied.

Herein, the objective of this thesis consists of two parts. The first part is to further validate the modified model. To do so, three different types of handsheets are made, low-pressing, medium pressing and high-pressing. To measure tensile strength, handsheets are cut to different notch size, then tensile strength data is fitted into the model and fracture characteristic length is extracted for further analysis. We also analyze the literature data against the model. The second part is to initiate the investigation of studying relationship between tensile strength and tear strength. The outcome of this study will guide people to fabricate paper materials with optimized tensile strength and tear strength.

2 Experimental

2.1 Handsheet preparation

Handsheets are prepared for tensile strength testing based on standard procedures. Specifically, a 305 square Nobile and Wood Handsheet former was used for making papers. Bleached Kraft Pulp (BKP) was used as raw materials for making handsheet. A Valley beater was used to beat the pulp and increase the packing of cellulose fibers. The sheet was prepared to 50 g/m^2 grammage. Pressing was also used to further strengthen the handsheet. Further drying under 50 ^{o}C oven to remove any water residue.

2.2 Tensile strength testing

Tensile strength of several prepared hand-sheets with varied grammage were tested to validate the LEFM model. The DENT was complete on an Instron model 3344 universal tester coupled with pneumatic clamping. The samples were cut into dimensions of length as 120 mm and width as 76 mm. The displacement rate of the tensile tester is set as 25.4 mm/min. Before the testing, the samples were aligned parallel to the clamps to avoid potential tearing effect.

3 Results

Figure 2 shows the tensile testing results for zero-notched samples of low, medium and high pressed handsheets. The results suggest that tensile strength of high-pressed handsheet is the highest (300 N) while handsheet undergoes low pressing has the lowest tensile strength (150 N). Interestingly, the maximum strain does not follow similar trend as tensile strength: high pressed > low pressed > medium pressed. This could attribute to the inherent flaw present within the network or it could be the fiber broken in the pressing process. The maximum strain for high-pressed sample is the largest while medium-pressed and low-pressed samples have relatively close strain ratio, suggesting the non-linearity behavior between pressing and maximum strain. Indeed, using high, medium and low to describe pressing can only provide qualitive information. Quantitative characterization such as pressing force or pressure are suggested to use for correlating strain with pressing conditions.

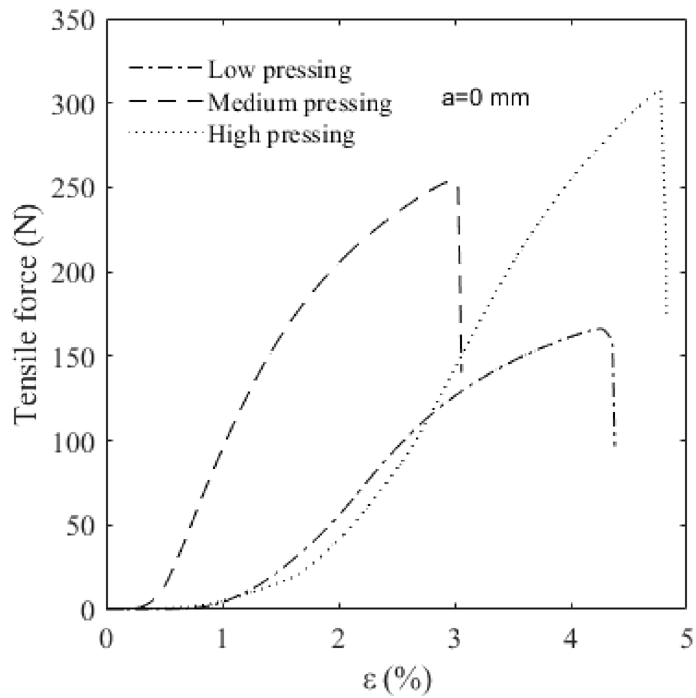

Figure 2. Tensile strength testing results: tensile forces as function of strain for a = 0 samples. The handsheets are pressed to level of low, medium and high.

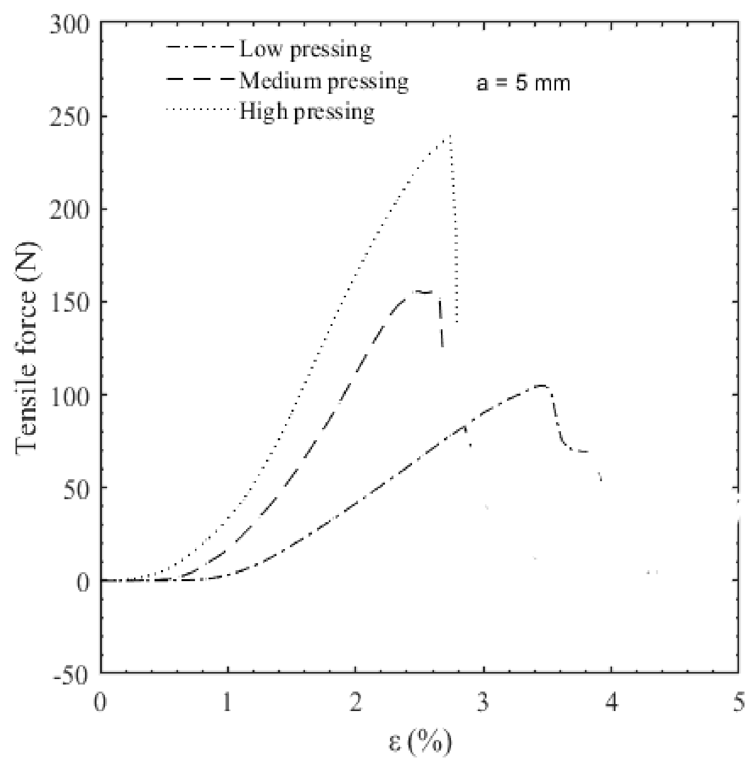

Figure 3. Tensile strength testing results: tensile forces as function of strain for a = 5 mm; samples. The handsheets are pressed to level of low, medium and high.

Figure 3 shows the tensile strength testing results for notch size as 5 mm. Similarly, the tensile strength (maximum force samples can withstand) is in the order of: high-pressed > medium-pressed > low-pressed. The high-pressed handsheets have the highest tensile strength of 250 N; the medium pressed sample has the tensile strength of around 150 N and the low-pressed sample has tensile strength of 110 N. The strain at which the handsheets break follows similar trend: high-pressed > medium-pressed > low-pressed (the low-pressed should shift to the left for around 1%).

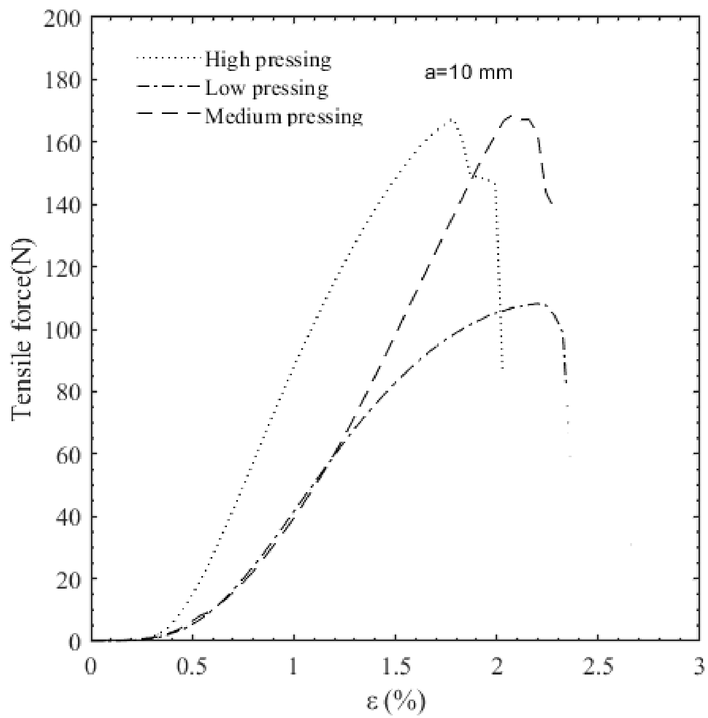

Figure 4. Tensile strength testing results: tensile forces as function of strain for a = 10 mm; samples. The handsheets are pressed to level of low, medium and high.

As sample notch increases to 10 mm, tensile strength for high-pressed handsheet drops to around 170 N. However, for medium-pressed sample, the tensile strength does not decrease so much and is around 160 N. This could be sample problem such as inherent cracks, fiber breaking down or poor fiber network formation. Tensile strength for low-pressed handsheets do not change much as well. And it is around 100 N. One of the observation is that the magnitude of tensile strength change under large notch size (>10 mm) is becoming insignificant. In contrast, under small notch size, the change is significant and can significantly reduce handsheet strength.

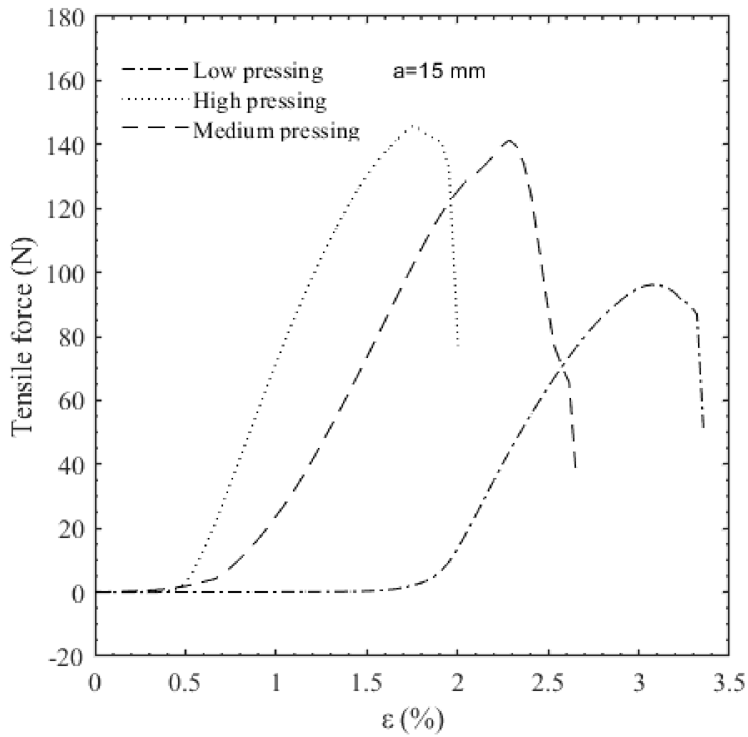

Figure 5. Tensile strength testing results: tensile forces as function of strain for a = 15 mm; samples. The handsheets are pressed to level of low, medium and high.

When the notch size reaches to 15 mm, tensile strength of high-pressed handsheet drops to 150 N, which is slightly higher than tensile strength of medium-pressed handsheet (139 N). The tensile strength for low-pressed handsheet decreases to around 90 N. those observations support the hypothesis that tensile strength changes becomes insignificant when notch sizes become large. The strain at which handsheet fails are similar (between 1.5-2%).

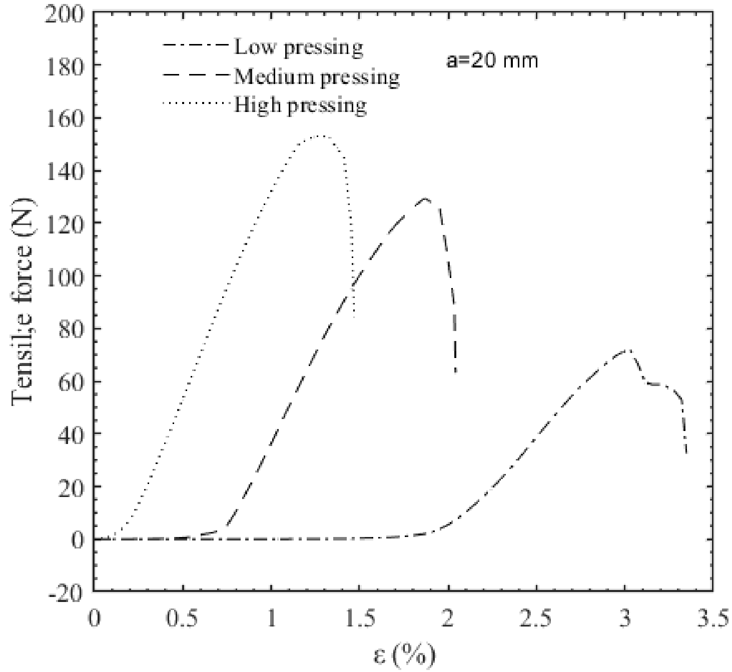

Figure 6. Tensile strength testing results: tensile forces as function of strain for a = 20 mm; samples. The handsheets are pressed to level of low, medium and high

In **Figure 6**, tensile strength of low-pressed sample drops to the lowest level (65 N). Tensile strength of medium-pressed sample decreases to around 125 N. For high-pressed handsheet, the tensile strength stays around 145 N.

4. Discussions

The relationship between paper materials tensile strength and tear strength indicates that fracture processing zone (FPZ) is a useful material property for optimizing paper processing manufacturing so that to obtain paper products with maximum tensile strength while maintaining high tear strength. The discussion section consists of two parts. The first part is to recast the LEFM and validate its application for paper materials. Once the modified linear fracture model is established, we use the model to evaluate literature data to extract fracture processing length. In the second part, we compared tensile strength and tear strength of paper and reveal how this fracture characteristic length affects tear strength.

4.1 Modified Linear Elastic Fracture Mechanic Model

The LEFM has a long history and success in solid materials such as metals and alloys and polymer materials. The feasibility of this model for fiber materials have some criticism mainly because fiber materials such as paper has varied strength depending on the packing and stacking of the fibers. This packing makes some properties un-predictable. Recently, Coffin [27] has modified this model by introducing a fracture processing zone, a parameter that has been an issue to obtain for paper and fiber materials. Studies by Coffin [27] has shown that the predicted tensile strength agrees well with experimental values.

In principal, many factors can affect the apparent tensile strength of paper or fiber materials, and those parameters mainly fall into two categories: microscopic property and macroscopic property. Microscopic property includes chemical composition of fibers, single fiber strength, fiber length and the "packing" of those fibers. The macroscopic property includes grammage, density and cracks within the material. For a given fibrous materials, the microscopic properties are fixed, but the macroscopic properties can be changed to increase or decrease the tensile strength.

Of those macroscopic properties, the cracks within the material or on the edge of papers is believed the main reason for materials failure under tensile testing. In the modified model, the role of this characteristic length is revealed. **Figure 6** shows the normalized tensile strength, e.g. actual tensile strength to maximum strength ratio (*T/F*) as a function of characteristic length. In general, **Figure 7** shows that tensile strength decreases as characteristic length increases. For materials with characteristic length less than 0.1-0.5 mm, the tensile strength is close to its maximum strength. This threshold value (0.1-0.5 mm) can be approximated as minimum zone length (d_0). Apparently, tensile strength is also sample size dependent. The dependence becomes significant once the sample characteristic length becomes large. For example, when the characteristic length is less than 15 mm, materials with varied sample length (15 mm – 75 mm) have similar tensile strength. However, when the characteristic length is greater than 15 mm, the tensile strength increases dramatically as sample size increases. The observation that tensile strength increases as sample size increases agrees with the fact that large samples have the ability to dissipate energy and enhance improves the materials strength. This also has been verified in experiment.[27]

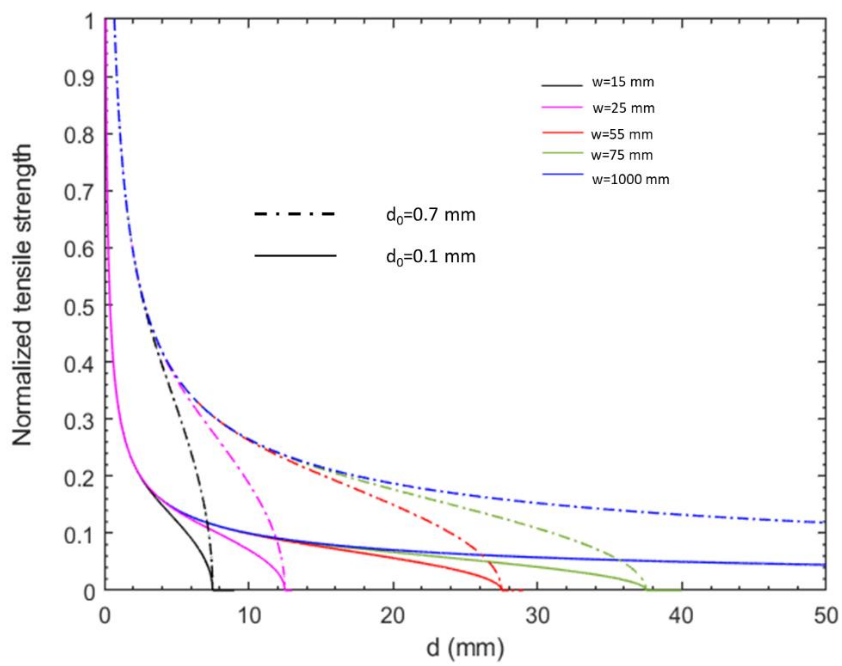

Figure 7. Predicted normalized tensile strength as function of characteristic length of double-edged notched paper sample (DENT).

4.2 Determination of Characteristic Length (d) of Prepared Handsheets

To compare all the data, tensile strength data under different pressing conditions and notch size are compiled in **Figure 8**. From **Figure 8**, it is concluded that a general trend that tensile strength decreases as notch size increases can be seen.

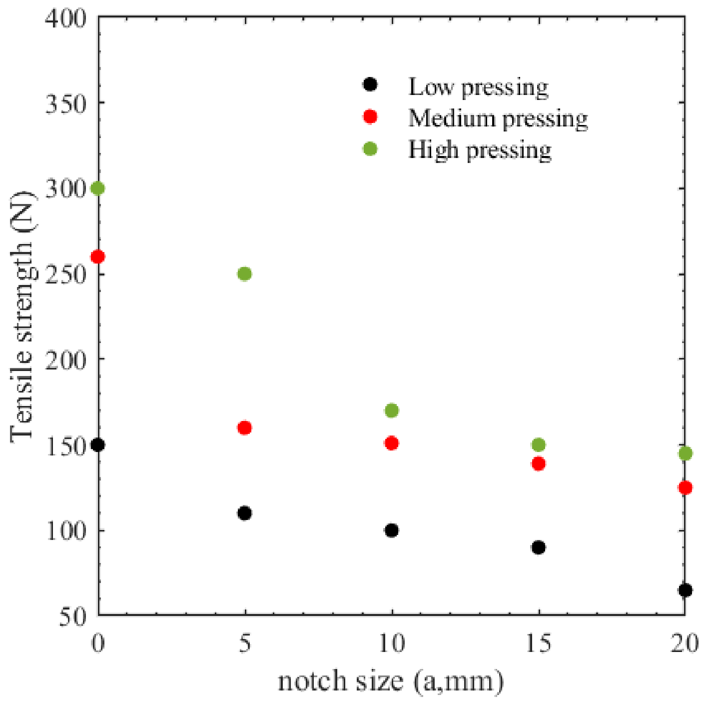

Figure 8. Tensile strength data compile: tensile strength as function of notch size for low-pressed, medium-pressed and high-pressed handsheets.

To determine the fracture characteristic length, the data in **Figure 9** was used and fitted into the modified LEFM model. The high-pressed handsheets shifts to the left to around 0.5 mm. The low-pressed handsheets were shifted to around 12 mm and the medium-pressed samples were shifted to left at the magnitude of 4 mm. After the data shifting, all the data can be fitted into the fracture model (black solid line), suggesting that the model works for the prepared handsheets. **Figure 9** indicates that all the data points follow similar trend and this trend is captured by the LEFM model.

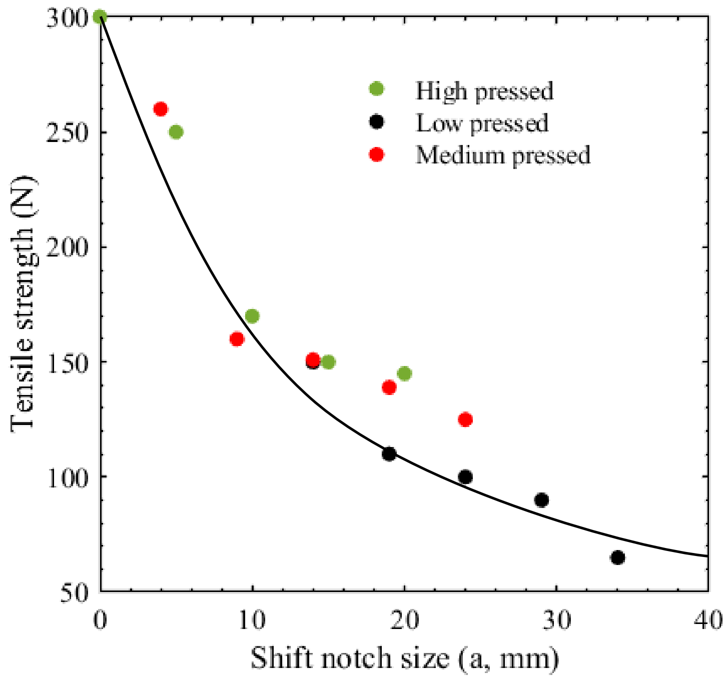

Figure 9. Tensile strength of handsheet as functions of shifted notch size for low-pressed, medium-pressed and high-pressed handsheets.

4.3 Determination of Characteristic Length (d) from Literature

Despite that the characteristic length in equations can be used for describing the inherent cracks length of paper materials, this characteristic length is often difficult to directly measure due to experimental limitations. One of the indirect way of obtaining this parameter is by combining the experimental data with this equation. It should be noted here that d is not the fitting parameter. The fitting procedure used in this study is simply a complementary approach in which experimental measurement is impossible.

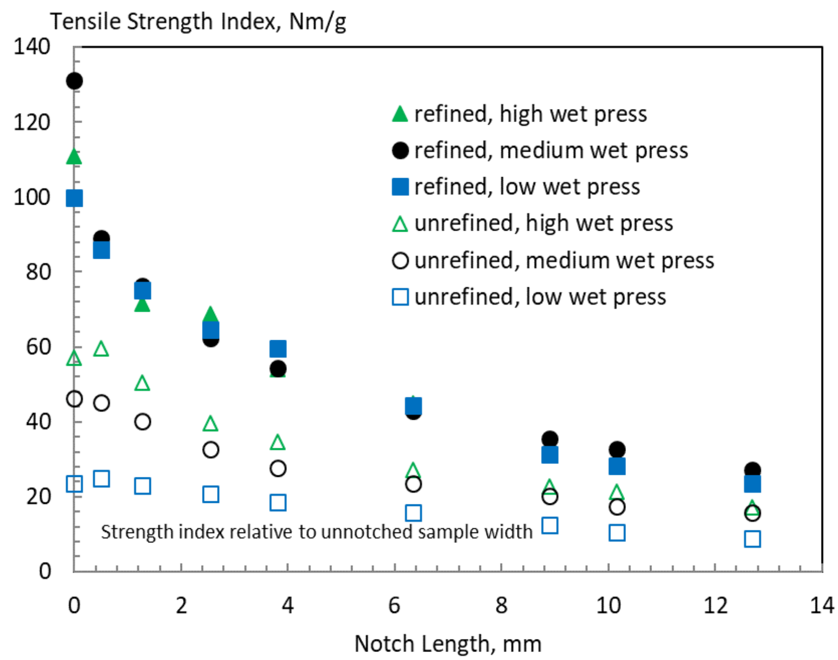

Figure 10. Raw tensile strength data extracted from Bither and Waterhouse on refining and wet-pressing on strength of paper.

Accordingly, literature data was obtained from Bither and Waterhouse [28] was extracted and shown in **Figure 10**. **Figure 10** shows the effect of notch size on tensile strength of handsheets under different processing. From **Figure 10**, we can see that we-pressing has minimal effect on tensile strength once the handsheets are refined. However, wet-pressing has significant effect on handsheet refining for un-refined handsheets. In general, the data from Bither and Waterhouse show that notch size can decrease tensile strength of handsheet, a conclusion that is also verified in modified linear elastic fracture model. It should be mentioned here that the notch size in **Figure 9** is not the characteristic length, but a size that is intentionally made in the study. To extract the characteristic length, the data in **Figure 10** is incorporated into equations to accommodate the modified characteristic length and the results are showed in **Figure 11**.

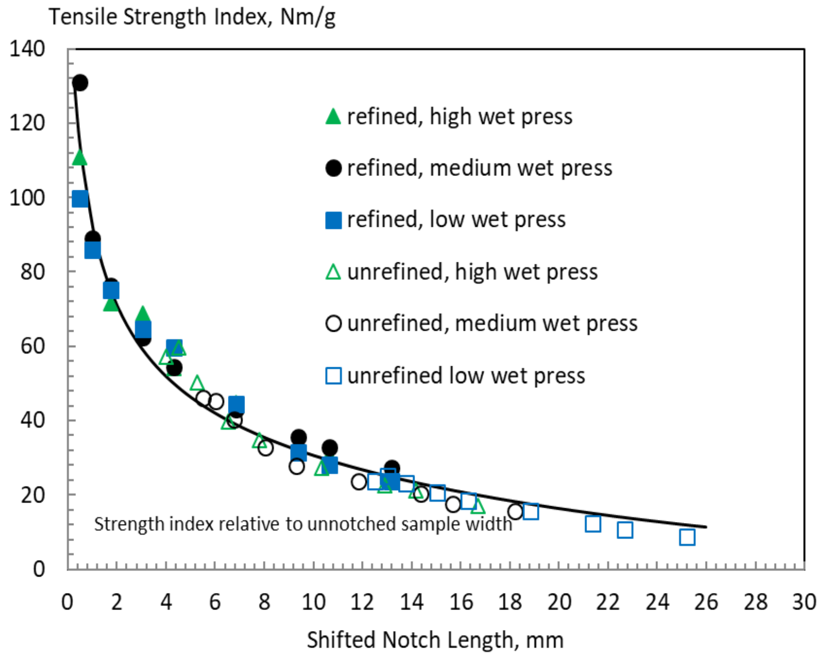

Figure 11. Shifted Bither and Waterhouse data to extract characteristic length.

Figure 11 shows that all the tensile strength data can be fitted into a universal modified linear elastic fracture model after the data was shifted to different values. This suggests that the modified model can work quite satisfying in terms of characterizing the characteristic length. The magnitude of the shift is shown in **Figure 12** bar chart. Not surprisingly, refined and high-wet pressed handsheets have the lowest characteristic length of around 0.7 mm. This lowest value is comparable with minimum fracture zone, which is often less than 1 mm. The highest shift, or characteristic length is the sample without refining and with low wet pressing. Interestingly, the characteristic length of refined handsheets are similar with values around 1 mm. However, for un-refined handsheets, the characteristic length varies from around 3 mm for high wet pressing handsheet to around 10 mm for low wet pressed handsheets. The high sensitivity of characteristic to wet-pressing under un-refined condition reveals the fact that water may serve as bridge for cellulose to form hydrogen bonds during the wet-pressing.[29]

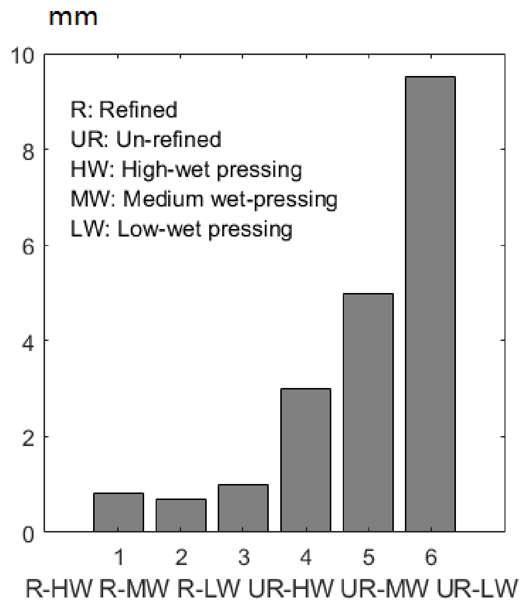

Figure 12. Characteristic length for handsheets undergo different process. Date was extracted from Bither and Waterhouse

The above analysis forms the experimental evidence that modified LEFM could be used for understanding the refining and wet pressing effect on tensile strength of handsheet paper.

4.4 Effect of Porosity on Fracture Characteristic Length

The ability of handsheet to consume tensile testing energy depends on the effectiveness of handsheet' s ability to quickly dissipate and spread the localized concentrated forces. In general, handsheets with more void space will have lower ability to concentrate force locally and thus less fracture sensitive relative to the tensile strength. Commonly, material with high density will have high tensile strength, assuming that the densification level is not large enough to break the fibers. Yet, the higher the density the more sensitive to cracks. Under this assumption, the correlation between porosity, a value to characterize the densification level of fiber network, and the fracture characteristic length will provide intuitive evidence for validating the modified LEFM theory.

Accordingly, two sets of analysis is presented here to support the above-mentioned hypothesis. Firstly, density data from Bither and Waterhouse[28]'s paper was extracted with corresponding characteristic fracture length (**Figure 4**). Then the porosity was determined by the following equation:

$$\Phi = 1 - \frac{\rho}{1500}$$

where ρ is the handsheet density; Φ is the porosity and 1500 is the maximum fiber wall density. The results in **Figure 5** consist of all the six data sets from Bither and Waterhouse[28] data. In general, as porosity increases, the fracture characteristic length increases. For low density handsheet which has porosity as high as 80%, the fracture characteristic length is as large as 10 mm. When the porosity is below 50%, the fracture characteristic length is somehow insensitive to the porosity or density, suggesting that there is threshold density above which the fracture characteristic length reaches the minimum value.

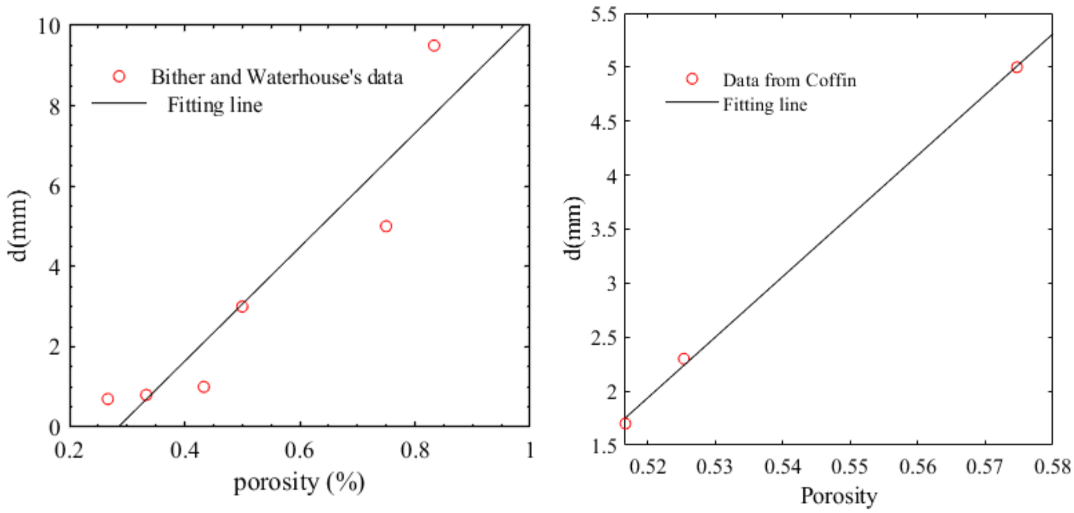

Figure 13. The effect of porosity on fracture characteristic length of Bither and Waterhouse's data (Left) and Coffin [27] data(Right)

The data on the right of **Figure 13** again shows the characteristic length as function of porosity for the handsheet prepared using pulp 8495 (Northern Bleached Kraft Pulp). Again, good correlation has been found between porosity and characteristic length. Notice that the sensitivity of characteristic length to porosity (or density) for these two data sets are different with Coffin's NBK more sensitive than Bither and Waterhouse's NSBK data. Clearly, the sensitivity is pump dependent. In general, the analysis again proves that the predicted or determined characteristic length from modified LEFM provides qualitive sense in terms of correlating density and tensile strength.

4.5 Modified Effective Tensile Strength Index

So far, tensile strength is characterized by the maximum force that handsheets can withstand before the fracture occurs. This maximum force is often useful from application standpoint. However, for handsheet testing purposes, this force can only provide the information of handsheet' s ability to withstand force, but not the fiber. Indeed, when the crack of the hand sheet increases to a large level, (>50% of the sample width), most of the forces are applied to the intact part of the sample rather than the whole width. In this sense, we created two different index to characterize handsheets ability to withstand forces:

$$index_a = \frac{T}{W}$$

$$index_b = \frac{T}{W - a}$$

where index_a is the traditional way to characterize the average stress in the unnotched region; and index_b is the modified index that characterizes the average stress in the notched region.

In **Table 1**, copy t paper was used as testing materials. The copy paper was cut based on the red-dot line represents the original method ($index_a$) while the blue-square line represents the modified tensile strength index ($index_b$).

From **Figure 14**, it can be seen that F/W decreases steadily as notch size increases, agreeing with the fact that large fracture or notch size can make copy paper unable to withstand large amount of force. As the notch size increases to around 36 mm, the copy paper has almost zero tensile strength. As the notch size reaches zero, the maximum tensile strength index is about 3.2 N/mm. It should be noted here that the zero-notch size does not really exist as there are always some small cracks at the edges of the sample.

Table 1. Tensile strength testing results and crack size for DENT for copy paper

Sample entry	Notch size (a, mm)	Tensile strength (T, N)
1	0	240
2	5	122
3	10	90
4	15	89
5	20	72
6	25	61
7	28	50
8	32	32
9	34	24
10	35	22
11	36	17
12	37	15

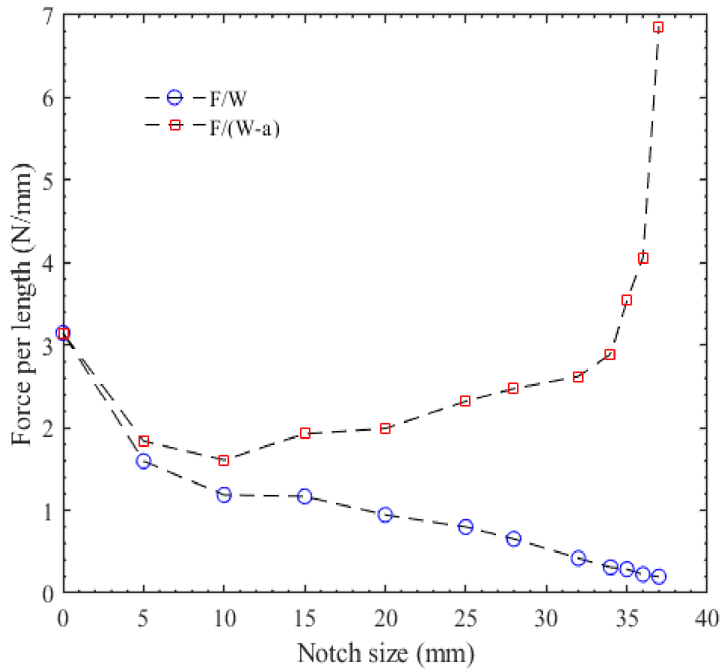

Figure 14. Comparison between two defined tensile strength index. The red square is the modified index while the blue dot is the original index.

Interestingly, the modified index, e.g. *F/(w-a)* decreases first and then dramatically increases. It decreases at beginning because the overall tensile strength decreases. As the notches size increase, most of the applied tensile forces are on the intact part, meaning that the modified tensile strength index approximates a few fibers' ability to hold the tensile forces. Ideally, when the intact length becomes the length of a few nanometers, the tensile strength would be the strength of single fibers. Indeed, as point out by some studies, the intrinsic tensile strength of paper or fiber materials are more than the measured tensile strength. It is the cracks or flaws of within the fiber network that reduces the strength of material. Therefore, it is suggested here that the modified tensile strength index can be an important parameter to characterize fibers tensile strength.

4.6 Tear strength and Tensile strength

The characteristic fracture length characterizes the ability of the network to store and concentrate strain energy. Larger fracture processing zones often leads to decreased ability to concentrate strain energy. Often, refining and wet-pressing are used for densification and improving tensile strength. The results in **Figure 15** shows the density of handsheet prepared from four different pulp as function of PFI milling time. From **Figure 15**, softwood pulp can form higher density of handsheet compared to hardwood pulp. This attributes to the fiber flexibility and ability to deform of softwood. Hardwood fibers tend to be stiff and inflexible. Thus, the density of hardwood prepared handsheets quickly reach maximum values under 4000 revs.

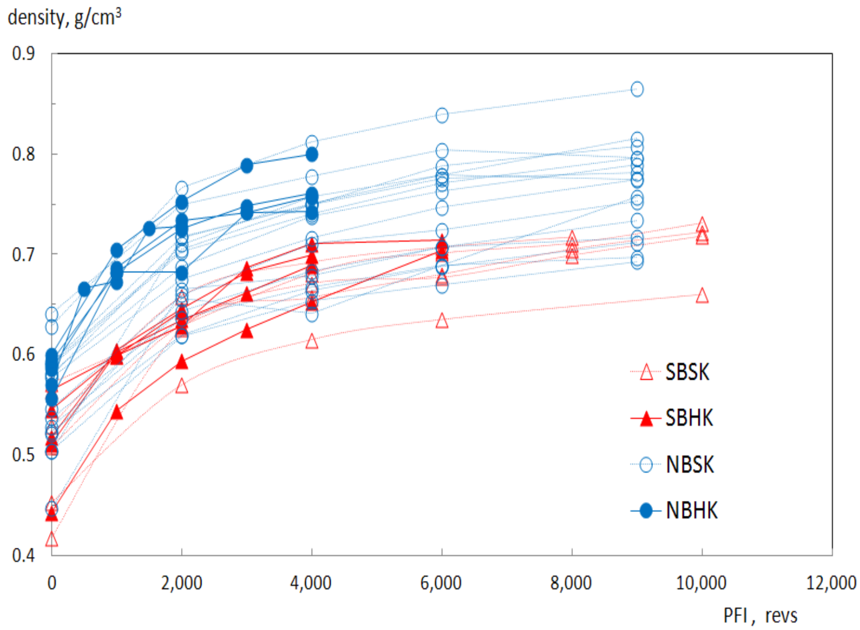

Figure 15. Handsheet density as a function of beating speed. SBSK: Southern bleached soft kraft; SBHK: southern bleached hardwood kraft; NBSK: northern bleached softwood kraft; NBHK: Northern bleached hardwood kraft. Data is from [30]

However, the refining or pressing level must be carefully controlled to avoid the fiber network breakdown and reduced tear strength. As shown by Coffin, the tear strength drops dramatically once the characteristic fracture length is less than fiber length.

Accordingly, literature tear index and breaking length data was extracted for four different pulp and shown in **Figure 16**, namely SBSK, SBHK, NBSK and NBHK. Interestingly, the relationship between breaking length and tear index is highly dependent on the pulp type. For example, for hardwood based handsheets, as density increases, the tensile strength or the breaking length keep increasing. However, the tear index increases first at low density. And then it drops dramatically once the breaking length drops below 5 km. This observation similar to Coffin's theoretical prediction that too much densification can lead to fibers breaking. This is due to that hardwood have low flexibility and it cannot conform itself to form a inter-connected fiber network. Instead, those stiff fiber is sensitive to the beating/refining and may be broken prior to forming handsheet, which leaves many cracks within the handsheet. Those cracks may not lead to reduced tensile strength as those fiber still has the ability to contain strain energy, but it may lead to reduced tear strength because of those cracks.

In contrast, for softwood prepared handsheet, as density increases, both the breaking length and tear index increase, indicating that softwood has high ability to form dense materials without sacrificing fiber strength.

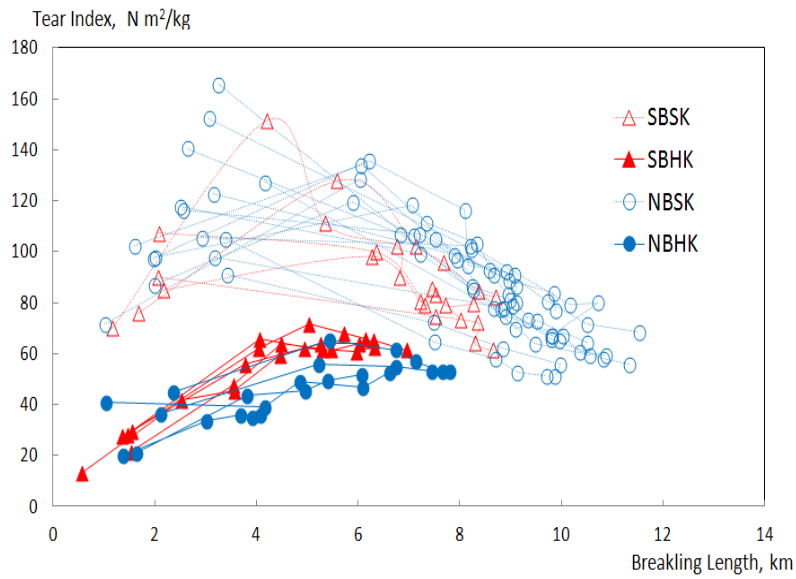

Figure 16. Handsheet tear index as a function of breaking length. SBSK: Southern bleached soft kraft; SBHK: southern bleached hardwood kraft; NBSK: northern bleached softwood kraft; NBHK: Northern bleached hardwood kraft. Data is from literature [30]

5. Conclusion

In this study, modified LEFM was validated using both literature data and prepared handsheets data. The results show that the model can be used for many purposes: first, the model can characterize handsheet or fiber materials' ability to withstand tensile loads. As shown in the study, handsheets undergoing different refining and pressing procedure yield materials with varied tensile strength. The model successfully captured those effects on the strength development. Secondly, the model can be used to qualifiedly or quantitatively determine or estimate the fracture processing zone. As shown in the analysis, a simple shift method coupled with data fitting can indirectly give the characteristic fracture length. This characteristic length parameter can be used for evaluating refining or wetting effect on tensile strength.

To further evaluate the importance of the determined characteristic fracture length, a correlation between porosity and characteristic length was found. The sensitivity of characteristic length to porosity or density is fiber-type dependent.

Based on the modified LEFM, we have invented a new tensile index. Instead of using the whole sample length, we divided the tensile strength by the intact part of the sample under tensile strength testing. Our results suggests that this modified tensile strength index can capture a few important aspects of materials strength: when the notch size is small compared to the sample size, the modified index agrees with fracture model; when the notch size is comparable to the sample size (> 50%), the modified tensile strength index increases dramatically. In the extreme case, if the intact part of the sample is in the magnitude of fiber length, then the modified tensile strength index can estimate the intrinsic tensile strength, which is significantly larger than apparent tensile strength.

Lastly, we evaluate the relationship between breaking length and tear strength using literature values. It is concluded that softwood based handsheets can have larger density, tear strength and tensile strength compared to hardwood based handsheets. When developing high strength fiber materials, it is recommended that the beating/refining/pressing should be not too strong to avoid the drastic drops of tear strength.

Reference

1. Yang, Q., et al., *Paper spray ionization devices for direct, biomedical analysis using mass spectrometry.* International journal of mass spectrometry, 2012. **312**: p. 201-207.
2. Tang, L., et al., *Preparation, structure, and electrochemical properties of reduced graphene sheet films.* Advanced Functional Materials, 2009. **19**(17): p. 2782-2789.
3. Khwaldia, K., E. Arab‐Tehrany, and S. Desobry, *Biopolymer coatings on paper packaging materials.* Comprehensive reviews in food science and food safety, 2010. **9**(1): p. 82-91.
4. Wang, C., et al., *High strength cellulose/ATT composite films with good oxygen barrier property for sustainable packaging applications.* Cellulose, 2018. **25**(7): p. 4145-4154.
5. Zheng, M., et al., *Effects of bentonite on physical, mechanical and barrier properties of cellulose nanofibril hybrid films for packaging applications.* Cellulose, 2019. **26**(9): p. 5363-5379.
6. Sehaqui, H., Q. Zhou, and L.A. Berglund, *Nanofibrillated cellulose for enhancement of strength in high-density paper structures.* Nord Pulp Pap Res J, 2013. **28**(2): p. 182-189.
7. Motamedian, H.R., A.E. Halilovic, and A. Kulachenko, *Mechanisms of strength and stiffness improvement of paper after PFI refining with a focus on the effect of fines.* Cellulose, 2019. **26**(6): p. 4099-4124.
8. Li, H., et al., *Surface modification of cellulose fibers with layer-by-layer self-assembly of lignosulfonate and polyelectrolyte: Effects on fibers wetting properties and paper strength.* Cellulose, 2012. **19**(2): p. 533-546.
9. Peng, L., Y. Meng, and H. Li, *Facile fabrication of superhydrophobic paper with improved physical strength by a novel layer-by-layer assembly of polyelectrolytes and lignosulfonates-amine.* Cellulose, 2016. **23**(3): p. 2073-2085.
10. Jacobs, N.T., et al., *Biaxial tension of fibrous tissue: using finite element methods to address experimental challenges arising from boundary conditions and anisotropy.* Journal of biomechanical engineering, 2013. **135**(2).
11. Cartz, L., *Nondestructive testing.* 1995.
12. Malhotra, V.M. and N.J. Carino, *Handbook on nondestructive testing of concrete*. 2003: CRC press.
13. Bray, D.E. and D. McBride, *Nondestructive testing techniques.* STIA, 1992. **93**: p. 17573.
14. Mark, R.E., J. Borch, and C. Habeger, *Handbook of physical testing of paper*. Vol. 1. 2002: Crc Press.
15. Facca, A.G., M.T. Kortschot, and N. Yan, *Predicting the tensile strength of natural fibre reinforced thermoplastics.* Composites Science and Technology, 2007. **67**(11-12): p. 2454-2466.
16. Tryding, J., *In-plane fracture of paper.* Division of Structural Mechanics, Lund Institute of Technology, 1996.
17. Niskanen, K., *Strength and fracture of paper.* Products of Papermaking, 1993. **2**: p. 641-725.

18. Mao, R., et al., *Comparison of fracture properties of cellulose nanopaper, printing paper and buckypaper.* Journal of Materials Science, 2017. **52**(16): p. 9508-9519.
19. Mäkelä, P., *On the fracture mechanics of paper.* Nordic Pulp & Paper Research Journal, 2002. **17**(3): p. 254-274.
20. Uesaka, T., et al., *Tearing resistance of paper and its characterization.* JAPAN TAPPI JOURNAL, 1979. **33**(6): p. 403-409.
21. Ferrill, D.A., K.J. Smart, and A.P. Morris, *Fault failure modes, deformation mechanisms, dilation tendency, slip tendency, and conduits v. seals.* Geological Society, London, Special Publications, 2020. **496**(1): p. 75-98.
22. Pak, Y., *Linear electro-elastic fracture mechanics of piezoelectric materials.* International Journal of Fracture, 1992. **54**(1): p. 79-100.
23. Atkinson, C., *On stress singularities and interfaces in linear elastic fracture mechanics.* International Journal of Fracture, 1977. **13**(6): p. 807-820.
24. Pan, E., *A general boundary element analysis of 2-D linear elastic fracture mechanics.* International Journal of Fracture, 1997. **88**(1): p. 41-59.
25. Pook, L.P., *Linear elastic fracture mechanics for engineers: theory and applications*. 2000: WIT press.
26. Clausing, D., *Crack stability in linear elastic fracture mechanics.* International Journal of Fracture Mechanics, 1969. **5**(3): p. 211-227.
27. Coffin, D.W., K. Li, and J. Li. *Utilization of modified linear elastic fracture mechanics to characterize the fracture resistance of paper*. in *15th Fundamental Research Symp., Cambridge, UK*. 2013.
28. Bither, T. and J. Waterhouse, *Strength development through refining and wet pressing.* Tappi journal, 1992. **75**(11): p. 201-208.
29. Belle, J. and J. Odermatt, *Initial wet web strength of paper.* Cellulose, 2016. **23**(4): p. 2249-2272.
30. Nanko, H., D. Hillman, and A. Button, *The World of Market Pulp [ressource Électronique]*. 2005: WOMP LLC.

Appendix
Tensile testing results for low-pressed handsheets

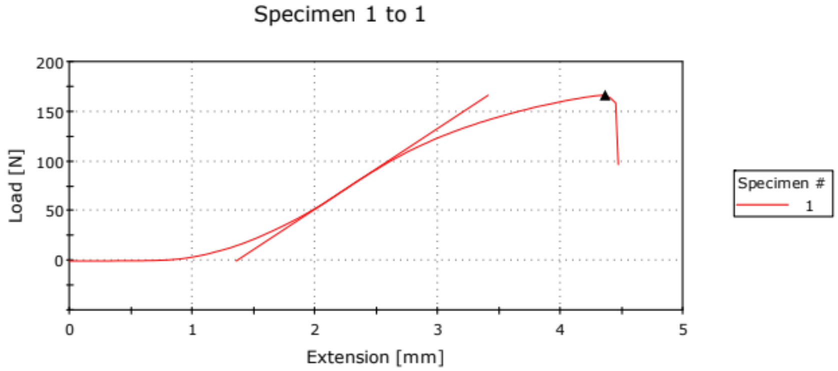

	Load at Tensile strength [N]	Tensile extension at Tensile strength [mm]	Maximum Slope (Automatic Young's) [N/mm]	Area under curve [J]
1	166.22443	4.36062	81.02499	-----

Figure 17.Low-pressing notch=0

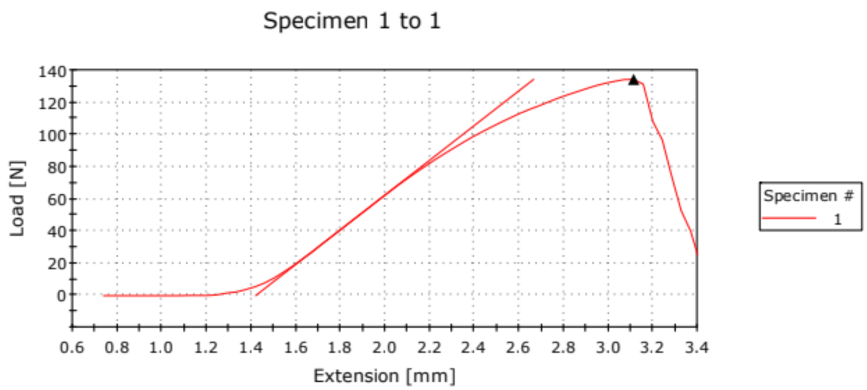

	Load at Tensile strength [N]	Tensile extension at Tensile strength [mm]	Maximum Slope (Automatic Young's) [N/mm]	Area under curve [J]
1	134.01064	3.11042	107.67643	-----

Figure 18.Low-pressing notch=5 mm

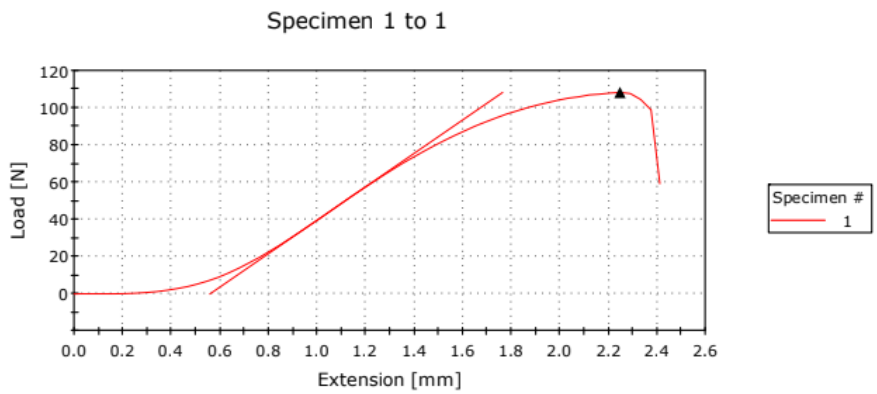

	Load at Tensile strength [N]	Tensile extension at Tensile strength [mm]	Maximum Slope (Automatic Young's) [N/mm]	Area under curve [J]
1	108.17231	2.24437	89.81721	0.11437

Figure 19.Low-pressing notch= 10 mm

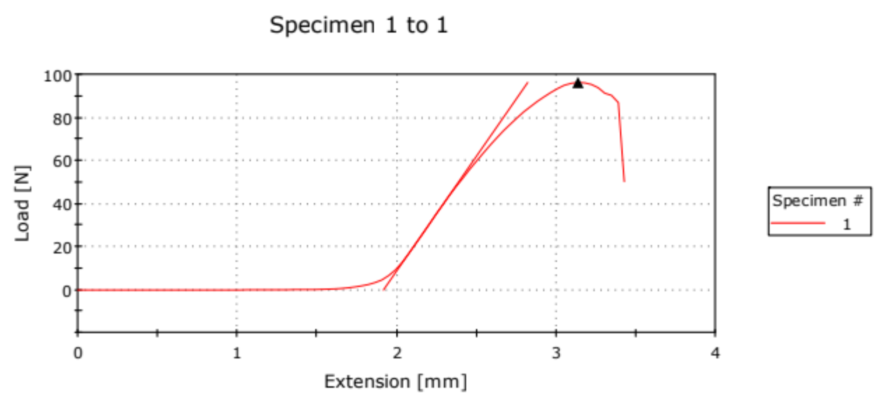

	Load at Tensile strength [N]	Tensile extension at Tensile strength [mm]	Maximum Slope (Automatic Young's) [N/mm]	Area under curve [J]
1	96.12976	3.13354	106.14839	0.07096

Figure 20.Low-pressing notch= 15 mm

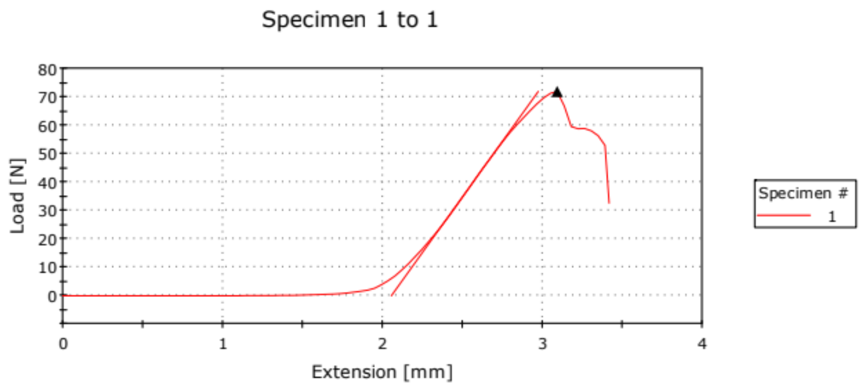

	Load at Tensile strength [N]	Tensile extension at Tensile strength [mm]	Maximum Slope (Automatic Young's) [N/mm]	Area under curve [J]
1	71.80585	3.09042	78.26945	0.04255

Figure 21.Low-pressing notch= 20 mm

Tensile testing results for medium-pressed handsheets

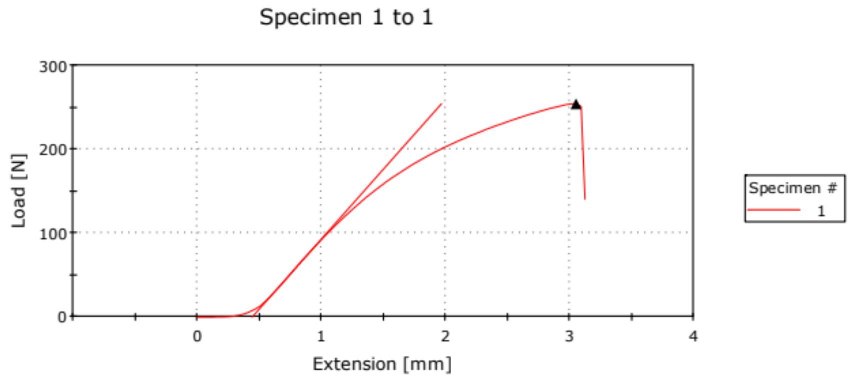

	Load at Tensile strength [N]	Tensile extension at Tensile strength [mm]	Maximum Slope (Automatic Young's) [N/mm]	Area under curve [J]
1	253.67346	3.04875	166.40536	0.42460

Figure 22.Medium-pressing notch=0

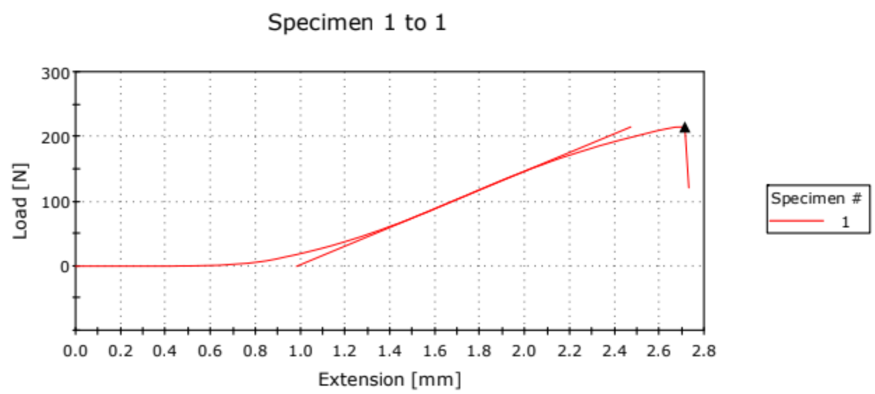

	Load at Tensile strength [N]	Tensile extension at Tensile strength [mm]	Maximum Slope (Automatic Young's) [N/mm]	Area under curve [J]
1	214.68085	2.70937	144.39903	0.21324

Figure 23.Medium-pressing notch= 5 mm

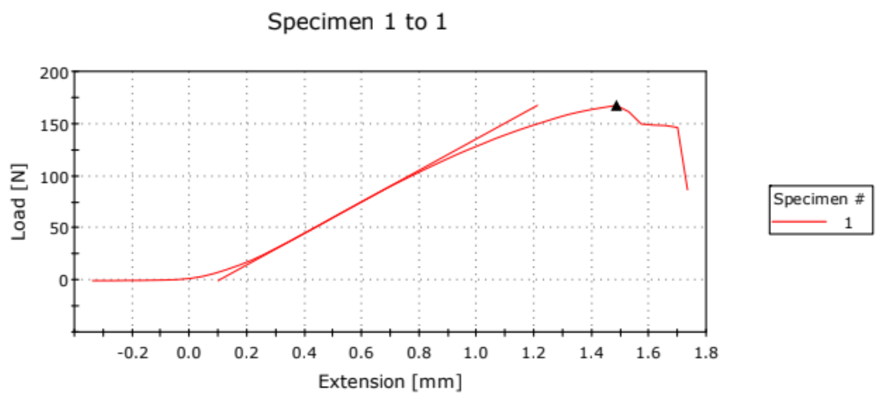

	Load at Tensile strength [N]	Tensile extension at Tensile strength [mm]	Maximum Slope (Automatic Young's) [N/mm]	Area under curve [J]
1	167.56624	1.48375	150.78974	0.13446

Figure 24.Medium-pressing notch= 10 mm

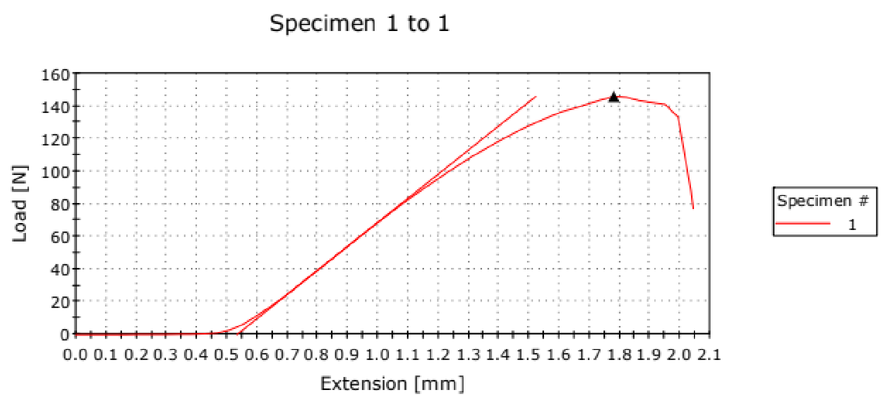

	Load at Tensile strength [N]	Tensile extension at Tensile strength [mm]	Maximum Slope (Automatic Young's) [N/mm]	Area under curve [J]
1	145.76436	1.77917	147.17631	0.10535

Figure 25.Medium-pressing notch= 15 mm

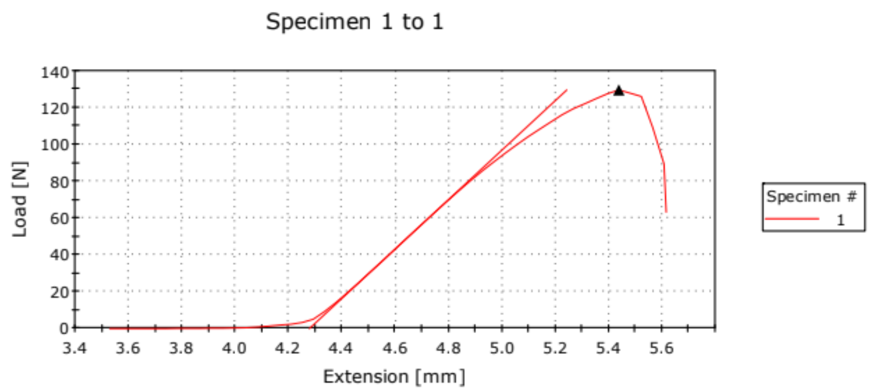

	Load at Tensile strength [N]	Tensile extension at Tensile strength [mm]	Maximum Slope (Automatic Young's) [N/mm]	Area under curve [J]
1	129.45386	5.43583	134.32761	-----

Figure 26.Medium-pressing notch = 20 mm

Tensile testing results for high-pressed handsheets

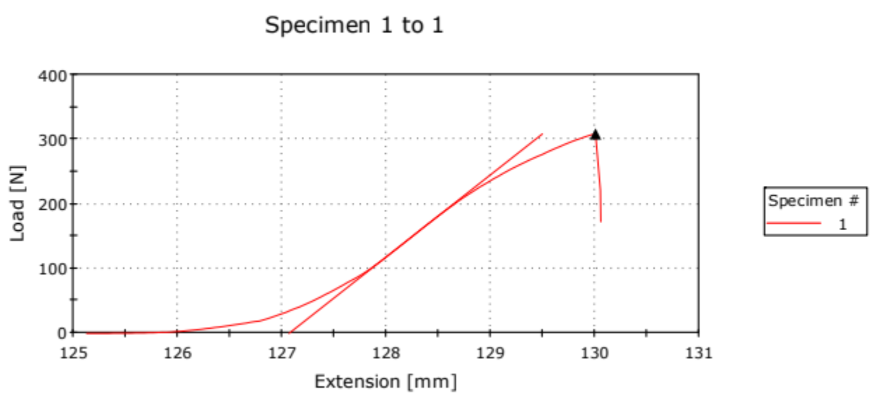

	Load at Tensile strength [N]	Tensile extension at Tensile strength [mm]	Maximum Slope (Automatic Young's) [N/mm]	Area under curve [J]
1	307.60770	130.00290	126.75048	-----

Figure 27.High-pressing notch=0

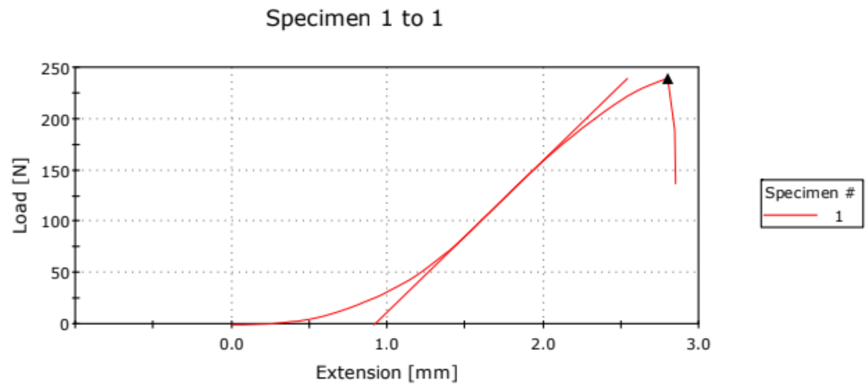

	Load at Tensile strength [N]	Tensile extension at Tensile strength [mm]	Maximum Slope (Automatic Young's) [N/mm]	Area under curve [J]
1	239.11623	2.79417	147.43584	0.26155

Figure 28.High-pressing notch=5 mm

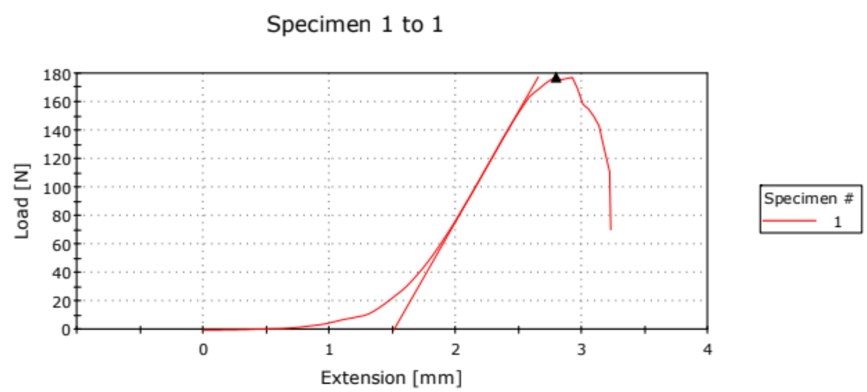

	Load at Tensile strength [N]	Tensile extension at Tensile strength [mm]	Maximum Slope (Automatic Young's) [N/mm]	Area under curve [J]
1	177.30119	2.79458	154.83256	0.13656

Figure 29.High-pressing notch= 10 mm

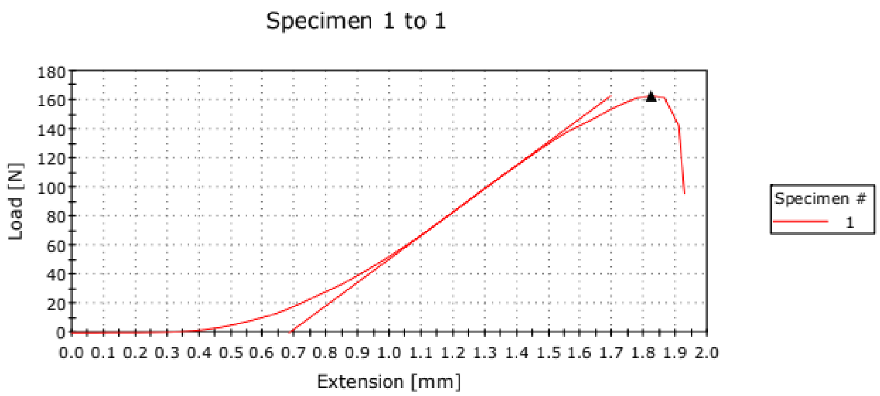

	Load at Tensile strength [N]	Tensile extension at Tensile strength [mm]	Maximum Slope (Automatic Young's) [N/mm]	Area under curve [J]
1	162.53329	1.82062	160.82983	0.10624

Figure 30.High-pressing notch= 15 mm

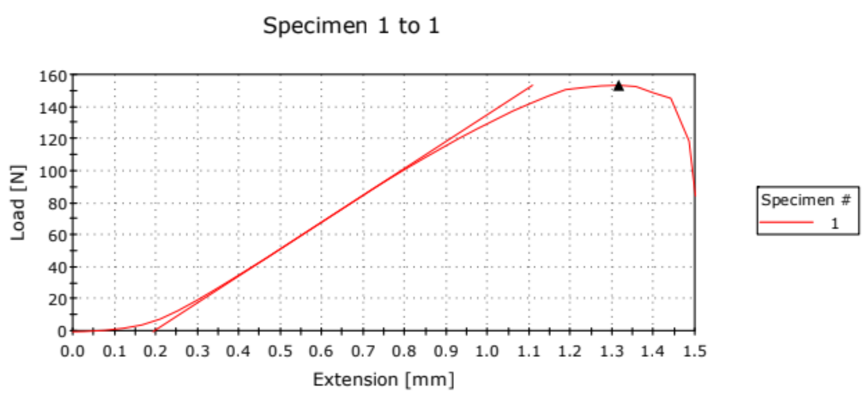

	Load at Tensile strength [N]	Tensile extension at Tensile strength [mm]	Maximum Slope (Automatic Young's) [N/mm]	Area under curve [J]
1	153.22189	1.31354	167.63262	0.10044

Figure 31.High-pressing notch= 20 mm